Available online at www.sciencedirect.com
SCIENCE DIRECT®
Journal of Organometallic Chemistry 680 (2003) 286–293
Journal of Organometallic Chemistry
www.elsevier.com/locate/jorganchem

Platination of [3-X-7,8-Ph_2-7,8-*nido*-$C_2B_9H_8$]$^{2-}$ (X = Et, F) Synthesis and characterisation of slipped and 1,2→1,7 isomerised products☆

Susan Robertson, David Ellis, Georgina M. Rosair, Alan J. Welch *

Department of Chemistry, Heriot-Watt University, Edinburgh EH14 4AS, UK

Received 25 February 2003; received in revised form 17 April 2003; accepted 17 April 2003

Dedicated to Professor M. Frederick Hawthorne on the occasion of his 75th birthday in recognition of his outstanding achievements in carborane and metallacarborane chemistry

Abstract

The reaction of the labelled carborane ligand [3-Et-7,8-Ph_2-7,8-*nido*-$C_2B_9H_8$]$^{2-}$ with a source of {$Pt(PMe_2Ph)_2$}$^{2+}$ affords non-isomerised 1,2-Ph_2-3,3-$(PMe_2Ph)_2$-6-Et-3,1,2-*closo*-$PtC_2B_9H_8$ (**1**). The analogous reaction between [3-F-7,8-Ph_2-7,8-*nido*-$C_2B_9H_8$]$^{2-}$ and {$Pt(PMe_2Ph)_2$}$^{2+}$ yields 1,8-Ph_2-2,2-$(PMe_2Ph)_2$-4-F-2,1,8-*closo*-$PtC_2B_9H_8$ (**3**). Compound **1** has a heavily slipped structure (Δ 0.72 Å), which to some degree obviates the need for C atom isomerisation. However, that it is a kinetic product of the reaction is evident from the fact that it reverts to isomerised 1,8-Ph_2-2,2-$(PMe_2Ph)_2$-4-Et-2,1,8-*closo*-$PtC_2B_9H_8$ (**2**) slowly at room temperature but more rapidly with gentle warming. The heteroatom and labelled-B atom positions in the isomerised compounds **2** and **3** may be explained most simply by the rotation of a CB_2 face of an intermediate based on the structure of **1**. Compounds **1**–**3** were characterised by a combination of spectroscopic and crystallographic techniques.

Keywords: Carborane; Metallacarborane; Isomerisation; Synthesis; Spectroscopy; Crystallographic study; Vertex labelling

1. Introduction

We are engaged in a programme of low-temperature isomerisations of metallacarboranes as models for the isomerisation of carboranes. Carborane isomerisation has been known for 40 years [1]. The *mechanism* of carborane isomerisation, however, remains poorly defined experimentally. In large measure, this is because such isomerisations only occur at high temperatures, meaning that vertex-labelling studies are unreliable [2]. However, Hawthorne's discovery of metallacarboranes [3], in which the {BH} fragment of a carborane is replaced by a metal fragment with which it is isolobal [4], afforded a new class of compounds that are good models for carboranes but which offer considerably more scope for electronic and steric modification. We have shown [5] that preparing a metallacarborane that is deliberately overcrowded can result in C-atom isomerisation which mimics the 1,2→1,7 isomerisation of $C_2B_{10}H_{12}$, either spontaneously or on mild heating. This, then, reawakens interest in vertex-labelling studies as mechanistic probes [6], and offers the opportunity to establish an experimental mapping of (hetero)carborane isomerisation to complement the numerous theoretical ideas advanced [7].

Following the synthesis of [3-Et-7,8-Ph_2-7,8-nido-$C_2B_9H_8$]$^{2-}$ [8], we showed [9] that its reaction with Ni(dppe)Cl_2 afforded not only the expected 1,2→1,2 C-atom isomerised product, but also an unexpected 1,2→1,7 C-atom isomerised species, the latter having a bearing on the 1,2→1,7 isomerisation of $C_2B_{10}H_{12}$. Using the labelled B vertex as a tag, we noted that the architecture of the 1,7 isomerised product most simply fitted with an isomerisation mechanism in which a CB_2

☆ Steric effects in heteroboranes. Part 29. For part 28 see Ref. [9].

* Corresponding author. Tel.: +44-131-451-3217; fax: +44-131-451-3180.
E-mail address: a.j.welch@hw.ac.uk (A.J. Welch).

0022-328X/03/$ - see front matter © 2003 Elsevier Science B.V. All rights reserved.
doi:10.1016/S0022-328X(03)00406-6

face of the presumed intermediate underwent a triangle face rotation (tfr). Since net 1,2→1,7 C-atom isomerisation in metallacarboranes tends to follow from platination [5] of a crowded *nido* carborane rather than nickelation [10], we were naturally interested in the reaction of [3-Et-7,8-Ph_2-7,8-*nido*-$C_2B_9H_8]^{2-}$ or its analogues with a source of $\{Pt(PR_3)_2\}^{2+}$. This paper reports the results of such reactions.

2. Experimental

2.1. Synthetic and spectroscopic studies

Experiments were performed under dry, oxygen-free, N_2 using standard Schlenk techniques, with some subsequent manipulation in the open laboratory. Solvents were freshly distilled over CaH_2 (CH_2Cl_2) or Na wire (THF, Et_2O, 40–60 petroleum ether) or stored over 4 Å molecular sieves ($CDCl_3$). NMR spectra at 200.13 (^{1}H), 128.38 (^{11}B), 161.98 MHz (^{31}P) or 376.50 MHz (^{19}F) were recorded on Bruker AC 200 or DPX 400 spectrometers from $CDCl_3$ solutions at ambient temperature, chemical shifts being recorded relative to $SiMe_4$ (^{1}H), $BF_3{\cdot}OEt_2$ (^{11}B), H_3PO_4 (^{31}P) or $CFCl_3$ (^{19}F). IR spectra were recorded from CH_2Cl_2 solutions on a Perkin–Elmer Spectrum RX FTIR spectrophotometer. Elemental analyses were determined by the departmental service. The starting [$HNMe_3$][3-Et-7,8-Ph_2-7,8-*nido*-$C_2B_9H_9$] [8], [$HNMe_3$][3-F-7,8-Ph_2-7,8-*nido*-$C_2B_9H_9$] [8] and *cis*-Pt(PMe_2Ph)$_2Cl_2$ [11] were prepared by literature methods or slight variants thereof. All other reagents were used as supplied.

2.1.1. Synthesis of 1,2-Ph_2-3,3-(PMe_2Ph)$_2$-6-Et-3,1,2-*closo*-$PtC_2B_9H_8$ (**1**)

[$HNMe_3$][3-Et-7,8-Ph_2-7,8-*nido*-$C_2B_9H_9$] (0.098 g, 0.26 mmol) in Et_2O (20 ml) was cooled to 0 °C and *n*-BuLi in hexanes (0.23 ml of 2.5 M solution ≡ 0.58 mmol) added. The solution was allowed to warm to room temperature, and then heated to reflux for 1 h, affording the salt Li_2[3-Et-7,8-Ph_2-7,8-*nido*-$C_2B_9H_8$]. Solvent was removed from this product, which was then redissolved in THF (20 ml) and frozen to −196 °C. Solid *cis*-Pt(PMe_2Ph)$_2Cl_2$ (0.143 g, 0.26 mmol) was added, and the mixture allowed to warm to room temperature under constant stirring, affording a yellow solution. The solvent was exchanged for CH_2Cl_2 and the product filtered through Celite®. Preparative TLC on silica using CH_2Cl_2/40–60 pet. ether as eluent (60:40) afforded one mobile band, recovered as an oily yellow/orange solid.

Compound **1**: Yield 0.040 g, 20%. Anal. Found: C, 48.0; H, 5.73. Calc. for $C_{32}H_{45}B_9P_2Pt$: C, 49.0; H 5.79%. IR ν (cm^{-1}): 2554 (br). ^{1}H-NMR δ (ppm): 7.6–7.0 (m, 20H, C_6H_5), 1.5–1.1 (m, 12H, PCH_3), 0.70 (t, 3H, CH_2CH_3), 0.58 (app t, 2H, CH_2CH_3). ^{11}B–{^{1}H}-NMR δ (ppm): 21.44 (1B), 4.64 (2B), −2.78 (2B), −4.07 (2B), −15.95 (2B). ^{31}P–{^{1}H}-NMR δ (ppm): −8.28 (br s, 2P, $^1J_{Pt-P} = 3064$ Hz).

2.1.2. Synthesis of 1,8-Ph_2-2,2-(PMe_2Ph)$_2$-4-Et-2,1,8-*closo*-$PtC_2B_9H_8$ (**2**)

Compound **1** slowly converts to a new species (**2**) on standing in solution at room temperature (close inspection of relatively uncluttered NMR spectra, e.g. ^{31}P, shows traces of **2** after several hours). Sufficient amounts of **2** for characterisation were afforded by heating **1** to reflux in THF. Although this conversion was never complete, and orange **1** and yellow **2** could not be separated by chromatography, **1** crystallises first and so could be removed.

Compound **2**: Anal. Found: C, 48.8; H, 5.80. Calc. for $C_{32}H_{45}B_9P_2Pt$: C, 49.0; H 5.79%. IR ν (cm^{-1}): 2556 (br). ^{1}H-NMR δ (ppm): 7.4–6.7 (m, 20H, C_6H_5), 1.7–1.3 (m, 12H, PCH_3), 0.5–0.4 (br unresolved m, 5H, CH_2CH_3). ^{11}B–{^{1}H}-NMR δ (ppm): −0.95 (2B), −5.53 (3B), −10.19 (1B), −13.06 (1B), −15.95 (1B), −22.41 (1B). ^{31}P–{^{1}H}-NMR δ (ppm): −14.69 (br unresolved d, 1P, $^1J_{Pt-P} = 3319$ Hz), −14.15 (br unresolved d, 1P, $^1J_{Pt-P} = 3290$ Hz), from highest frequency satellite $^2J_{P-P} \approx 21$ Hz.

2.1.3. Synthesis of 1,8-Ph_2-2,2-(PMe_2Ph)$_2$-4-F-2,1,8-*closo*-$PtC_2B_9H_8$ (**3**)

In a procedure similar to that described in Section 2.1.1, [$HNMe_3$][3-F-7,8-Ph_2-7,8-*nido*-$C_2B_9H_9$] (0.106 g, 0.29 mmol) was converted to its Li^+ salt and treated with *cis*-Pt(PMe_2Ph)$_2Cl_2$ (0.158 g, 0.29 mmol). Preparative TLC (CH_2Cl_2/40–60 pet. ether, 1:1) afforded a single mobile band, compound **3**, recovered as a yellow solid.

Compound **3**: Yield 0.035 g, 16%. Anal. Found: C, 44.5; H, 5.11. Calc. for $C_{30}H_{38}B_9FP_2Pt{\cdot}0.6CH_2Cl_2$: C, 44.7; H 4.80%. IR ν (cm^{-1}): 2562 (br). ^{1}H-NMR δ (ppm): 7.5–7.0 (m, 20H, C_6H_5), 1.7–1.45 (m, 12H, PCH_3). ^{11}B–{^{1}H}-NMR δ (ppm): −0.42 (unresolved d, 1B, $^1J_{F-B} \approx 45$ Hz, B4), −2.49 (2B), −6.87 (1B), −14.35 (4B), −23.71 (1B). ^{31}P–{^{1}H}-NMR δ (ppm): −15.06 (s, 2P, $^1J_{Pt-P} = 3259$ Hz). ^{19}F-NMR δ (ppm): −209.5 (partially resolved q, $^1J_{F-B} \approx 39$ Hz).

2.2. Crystallographic studies

Single, diffraction-quality, crystals were grown by diffusion of a CH_2Cl_2 solution of compounds **1**, **2** and **3**, and a 5-fold excess of 40–60 petroleum ether at room temperature. Diffraction data were measured at 160(2) K on a Bruker AXS *P*4 diffractometer equipped with an Oxford Cryosystems Cryostream cooler. One asymmetric fraction of intensity data was collected [12] to $\theta_{max} = 25°$ with graphite-monochromated Mo–K_α ra-

diation ($\lambda = 0.71069$ Å) using ω-scans. Standard reflections were re-measured every 100 data and any crystal decay corrected. Data were corrected for absorption by ψ-scans. All structures were solved [13] by direct and difference Fourier methods and refined by full-matrix least-squares against F^2, with non-hydrogen atoms assigned anisotropic displacement parameters. Crystals of **3** become opaque after several minutes in air by loss of solvate. Freshly grown crystals contain $1\frac{3}{4}$ molecules of CH_2Cl_2 of solvation per molecule of **3**, comprising one ordered molecule and two fractionally ($\frac{1}{2}$ and $\frac{1}{4}$) ordered molecules. For the last two C–Cl was restrained to 1.70(5) Å in the refinement, and for the $\frac{1}{4}$ molecule refinement was isotropic only. H atom positions were calculated and allowed to ride during refinement (C–H distances 0.95 Å [phenyl], 0.99 Å [methylene] and 0.98 Å [methyl], B–H distances 1.12 Å) with displacement parameters calculated as 1.2, 1.2, 1.5 and 1.2 times the bound atom U_{eq}, respectively. The only exception to this was **2**, where H atoms bound to B were allowed to refine positionally although restrained to a B–H distance of 1.12(2) Å with free thermal refinement. Table 1 lists details of unit cell data, intensity data collection and structure refinement.

3. Results and discussion

3.1. Synthesis and spectroscopy

The reaction between [3-Et-7,8-Ph_2-7,8-*nido*-$C_2B_9H_8]^{2-}$ and *cis*-$Pt(PMe_2Ph)_2Cl_2$ in THF affords the orange compound 1,2-Ph_2-3,3-$(PMe_2Ph)_2$-6-Et-3,1,2-*closo*-$PtC_2B_9H_8$ (**1**) in moderate yield (not optimised) following work-up involving preparative TLC. Compound **1** was initially characterised by microanalysis, and IR and multinuclear NMR spectroscopy.

The $^{11}B–\{^1H\}$-NMR spectrum of **1** reveals five fairly broad peaks, 1:2:2:2:2 from high to low frequency. The chemical shift range, +22 to −16 ppm, is consistent with a formally *closo* although slipped platinacarborane [5], and the pattern of integrals suggests that the C_s symmetry of the ligand precursor has been maintained. However, the relative broadness of the resonances meant it was not possible to identify which arose from the Et-substituted B atom in the ^{11}B-NMR spectrum. The $^{31}P–\{^1H\}$-NMR spectrum contains only a singlet with platinum satellites ($^1J_{Pt-P} = 3064$ Hz), meaning either that the P atoms are symmetrically disposed or that the $\{PtP_2\}$ unit undergoes rotation about the Pt-cage axis which is rapid on the NMR timescale. In the ^1H-NMR spectrum are the expected resonances for C_6H_5 protons, a multiplet around 1–1.5 ppm due to pairs of prochiral Me groups and $^2J_{P-H}$ coupling, and at lower frequency a triplet and apparent triplet due to the Et group, the last a consequence of the adjacent carborane cage [8,9].

The nature of compound **1** was unambiguously established by a single-crystal diffraction study. Fig. 1 hosts a perspective view of a single molecule and Table 2 lists selected molecular parameters. Compound **1** is a *non-isomerised* 6-Et-3,1,2-PtC_2B_9 platinacarborane in which the $\{Pt(PMe_2Ph)_2\}$ fragment has nonetheless undergone a significant slippage distortion to relieve otherwise untenable steric crowding with the cage Ph groups. The structural confirmation of **1** is important, in that we have previously assumed [6,14] that the initial product of platination of a 7,8-Ph_2-7,8-*nido*-C_2B_9 ligand was indeed a 3,1,2-PtC_2B_9 species which then underwent isomerisation, but this is the first time such an initial product has been isolated. The $\{PtP_2\}$ unit is slipped [15] ca. 0.72 Å away from C1C2, considerably more than the corresponding distortion, ca. 0.42 Å, in 3,3-$(PEt_3)_2$-3,1,2-*closo*-$PtC_2B_9H_{11}$ [15], further illustrating that crowded diphenyl metallacarboranes exhibit enhanced structural distortions relative to analogues with no Ph groups attached to the cage C atoms [16]. As a consequence of this slipping, the Pt···C distances are very extended, 2.857(10) Å to C1 and 2.805(10) Å to C2, and are not included in Fig. 1.

The distortion in compound **1** is not restricted to slipping of the $\{PtP_2\}$ unit. The Ph rings on the cage C atoms are both twisted from their conformations in [3-Et-7,8-Ph_2-7,8-*nido*-$C_2B_9H_9]^-$ [8] to accommodate the steric demands both of the phosphine ligands on Pt and the Et label on B6. As we have noted, the orientations of Ph groups on C-adjacent diphenylcarboranes are conveniently described by the angle θ_{Ph}, defined [17] as the modulus of the average $C_{cage}–C_{cage}–C_{Ph}–C_{Ph}$ torsion angle. In [3-Et-7,8-Ph_2-7,8-*nido*-$C_2B_9H_9]^-$ [8], the Ph rings are disrotated to θ_{Ph} values of 12.9° and 24.1° to accommodate the Et substituent on B6. In **1**, the Ph rings are conrotated to subtend θ_{Ph} values of 43.6° (ring on C2) and 64.2° (ring on C1), the latter reflecting the fact that the Et substituent is angled to lie underneath C1. These are some of the highest θ_{Ph} values recorded. In non-slipped 3,1,2-MC_2B_9 diphenylmetallacarboranes, high θ_{Ph} values frequently result in partially opened, pseudo-*closo* structures [18] characterised by C1···C2 distances in excess of 2.4 Å. In **2**, however, a pseudo-*closo* distortion is obviated by the slipping away of the $\{PtP_2\}$ fragment, and the C1–C2 distance is short, 1.530(13) Å, reminiscent of the C–C distance in 7,8-*nido*-C_2B_9 carboranes. In fact, the C–C distance in **1** is actually shorter than that in [3-Et-7,8-Ph_2-7,8-*nido*-$C_2B_9H_9]^-$ [8] [1.602(3) Å, average $\theta_{Ph} = 18.5°$] and in [7,8-Ph_2-7,8-*nido*-$C_2B_9H_{10}]^-$ [19] [1.590(5) Å, average $\theta_{Ph} = 7.8°$ in $[HNEt_3]^+$ salt; 1.602(3) Å, average $\theta_{Ph} = 19.0°$ in $[C_6H_5CH_2NMe_3]^+$ salt], providing support for the suggestion [20] that the C–C bond strength increases

Table 1
Crystallographic data for compounds **1**, **2** and **3**·$1\frac{3}{4}CH_2Cl_2$

	1	**2**	**3**·$1\frac{3}{4}CH_2Cl_2$
Formula	$C_{32}H_{45}B_9P_2Pt$	$C_{32}H_{45}B_9P_2Pt$	$C_{30}H_{40}B_9FP_2Pt\cdot 1\frac{3}{4}CH_2Cl_2$
M_r	784.00	784.00	922.56
Colour	orange	yellow	yellow
Habit	block	block	plate
Crystal system	monoclinic	monoclinic	monoclinic
Space group	$P2_1/c$	$P2_1/n$	$P2_1/n$
Unit cell dimensions			
a (Å)	21.060(7)	9.2589(16)	12.547(2)
b (Å)	9.474(3)	28.113(9)	10.7074(19)
c (Å)	17.546(9)	13.729(3)	30.850(4)
α (°)	90	90	90
β (°)	101.93(4)	104.267(12)	95.379(14)
γ (°)	90	90	90
U (Å^3)	3425(2)	3463.3(14)	4126.3(11)
Z	4	4	4
D_{calc} (Mg m^{-3})	1.520	1.504	1.485
μ(Mo–K$_\alpha$) (mm^{-1})	0.421	0.417	0.373
F(0 0 0)	1560	1560	1822
Crystal size (mm^3)	0.72 × 0.48 × 0.24	0.58 × 0.38 × 0.28	0.42 × 0.30 × 0.14
Trans. factors	0.215–0.781	0.506–0.943	0.479–0.729
Data collected	6602	7549	9216
Ind. data, n	5346	6069	7207
R_{int}	0.0624	0.0338	0.0429
No. variables, p	397	429	469
R, wR_2 (all data)	0.0787, 0.1695	0.0327, 0.0746	0.0607, 0.0990
S (all data)	1.040	1.049	1.037
a, b	0.09, 55.35	0.03, 7.06	0.04, 7.33
E_{max}, E_{min} (e Å^{-3})	2.804, −3.081	0.796, −0.883	1.527, −0.736

$R = \Sigma||F_o|-|F_c||/\Sigma|F_o|$, $wR_2 = [\Sigma[w(F_o^2-F_c^2)^2]/\Sigma w(F_o^2)^2]^{1/2}$, where $w^{-1} = [\sigma^2(F_o)^2+(aP)^2+bP]$ and $P = [0.333(F_o)^2+0.667(F_c)^2]$, $S = [\Sigma[w(F_o^2-F_c^2)^2]/(n-p)]^{1/2}$, where n is the number of data and p the number of parameters.

as θ_{Ph}, at least until intolerably large θ_{Ph} values are reached.

The fact that compound **1** has accommodated its significant overcrowding by severe slipping rather than isomerisation is somewhat surprising [6]. However, in solution at room temperature, **1** clearly converts to a new, yellow, species, **2**, with very different spectral characteristics. Sufficient amounts of **2** for complete characterisation are afforded by heating **1** to reflux in THF. Although by this method the conversion of **1** → **2** is never quantitative, and **1** and **2** proved impossible to separate chromatographically, pure **2** could easily be obtained by fractional crystallisation which removed **1** first.

Compound **2** proved to be the anticipated 1,7 C-atom isomerised platinacarborane. The ^{11}B-NMR spectrum shows evidence of asymmetry with resonances in the ratio 2:3:1:1:1:1 from high to low frequency, the integral 3 resonance including a low-frequency shoulder due to 1B. Again, it was not possible to assign the resonance due to the Et-bound B atom, except to note that it is clearly not the lowest frequency one (−22.4 ppm). The ^{31}P–{^{1}H}-NMR spectrum indicates inequivalent P environments with $^2J_{P-P}$ measured on the highest frequency Pt satellite at ca. 21 Hz. It was not possible to resolve the CH_2 and CH_3 ethyl resonances in the ^{1}H-NMR spectrum measured at 200 MHz, these appearing as an ill-defined multiplet of overall integral 5 centred around 0.45 ppm.

A crystallographic study of **2** (Fig. 2 and Table 3) revealed a 1,8-Ph_2-2,2-$(PMe_2Ph)_2$-4-Et-2,1,8-*closo*-$PtC_2B_9H_8$ architecture. The cage has undergone isomerisation such that its C atoms are no longer adjacent, but separated by the B3–B4 connectivity, B4 carrying the Et label. The Pt atom is bound to a B_4C face, but is slipped by ca. 0.41 Å away from C1, affording Pt–B distances between 2.2 and 2.3 Å and a Pt–C1 distance of 2.628(4) Å. Thus compound **2** is analogous to the previously characterised species 1,8-Ph_2-2,2-$(PMe_2Ph)_2$-2,1,8-*closo*-$PtC_2B_9H_9$ [5,21] which has the same structure save for the Et label and very similar molecular dimensions [Δ 0.36 Å, Pt–C1 2.610(5) Å]. It is also related to the nickelacarborane 1,8-Ph_2-2-dppe-4-Et-2,1,8-*closo*-$NiC_2B_9H_8$ [9] formed as a minor product in the nickelation of [3-Et-7,8-Ph_2-7,8-*nido*-$C_2B_9H_8]^{2-}$.

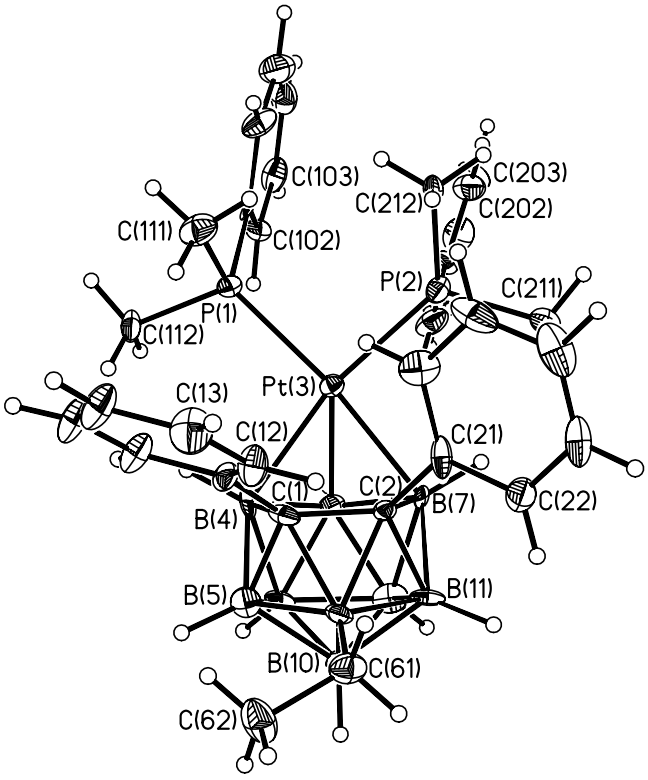

Fig. 1. Perspective view of compound **1**. Thermal ellipsoids are drawn at the 50% probability level, except for H atoms.

Seeking further information on the nature of the products of platination of 3-labelled-7,8-*nido*-diphenylcarborane, the fluoro-substituted anion [3-F-7,8-Ph_2-7,8-*nido*-$C_2B_9H_8$]$^{2-}$ was treated with *cis*-$Pt(PMe_2Ph)_2Cl_2$ in THF. Work-up involving TLC afforded one mobile product, the yellow species **3**, in modest yield.

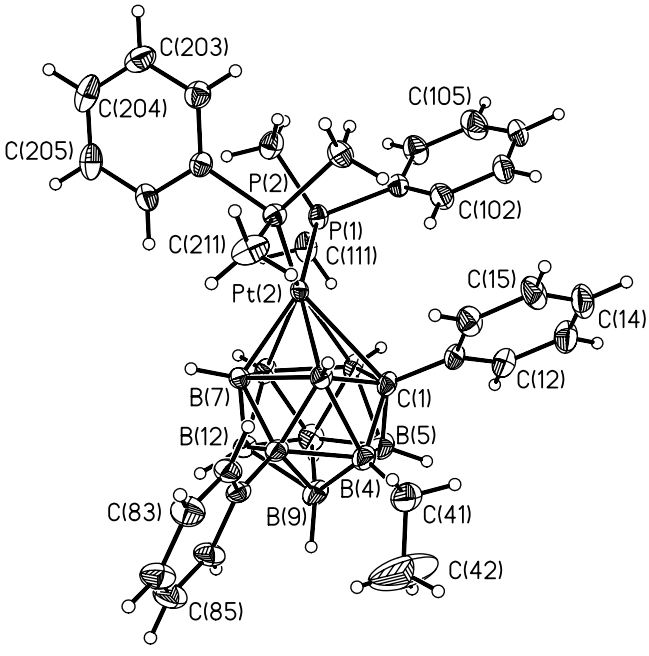

Fig. 2. Perspective view of compound **2**. Thermal ellipsoids are drawn at the 50% probability level, except for H atoms.

Table 2
Selected interatomic distances (Å) and interbond angles (°) for **1**

Bond lengths			
Pt(3)···C(1)	2.857(10)	B(7)–B(12)	1.850(17)
Pt(3)···C(2)	2.805(10)	B(7)–B(8)	1.834(16)
Pt(3)–B(7)	2.269(11)	B(8)–B(9)	1.765(16)
Pt(3)–B(8)	2.164(12)	B(8)–B(12)	1.792(18)
Pt(3)–B(4)	2.294(11)	B(9)–B(10)	1.778(16)
C(1)–C(2)	1.530(13)	B(9)–B(12)	1.773(18)
C(1)–B(4)	1.803(15)	B(10)–B(11)	1.778(16)
C(1)–B(5)	1.652(15)	B(10)–B(12)	1.760(17)
C(1)–B(6)	1.730(15)	B(11)–B(12)	1.771(17)
C(2)–B(6)	1.739(14)	B(6)–C(61)	1.583(16)
C(2)–B(11)	1.682(15)	C(61)–C(62)	1.529(15)
C(2)–B(7)	1.807(16)	Pt(3)–P(1)	2.281(3)
B(4)–B(5)	1.800(17)	Pt(3)–P(2)	2.292(3)
B(4)–B(9)	1.804(16)	P(1)–C(101)	1.811(11)
B(4)–B(8)	1.771(17)	P(1)–C(111)	1.823(12)
B(5)–B(6)	1.793(17)	P(1)–C(112)	1.814(10)
B(5)–B(10)	1.795(17)	P(2)–C(201)	1.808(11)
B(5)–B(9)	1.780(17)	P(2)–C(211)	1.806(11)
B(6)–B(10)	1.777(17)	P(2)–C(212)	1.817(11)
B(6)–B(11)	1.778(17)	C(1)–C(11)	1.514(15)
B(7)–B(11)	1.811(15)	C(2)–C(21)	1.511(14)
Bond angles			
C(11)–C(1)–C(2)	124.2(9)	P(1)–Pt(3)–P(2)	93.48(9)
C(11)–C(1)–B(6)	117.2(9)	Pt(3)–P(1)–C(101)	116.2(3)
C(11)–C(1)–B(5)	115.6(8)	Pt(3)–P(1)–C(111)	115.1(4)
C(11)–C(1)–B(4)	117.5(9)	Pt(3)–P(1)–C(112)	114.5(4)
C(21)–C(2)–C(1)	123.5(9)	C(101)–P(1)–C(111)	106.1(5)
C(21)–C(2)–B(6)	123.4(8)	C(101)–P(1)–C(112)	100.9(5)
C(21)–C(2)–B(11)	119.6(8)	C(111)–P(1)–C(112)	102.2(6)
C(21)–C(2)–B(7)	111.5(7)	Pt(3)–P(2)–C(201)	109.5(3)
C(61)–B(6)–C(1)	126.7(10)	Pt(3)–P(2)–C(211)	118.6(4)
C(61)–B(6)–C(2)	124.3(9)	Pt(3)–P(2)–C(212)	118.7(3)
C(61)–B(6)–B(11)	123.2(9)	C(201)–P(2)–C(211)	101.7(5)
C(61)–B(6)–B(10)	124.9(9)	C(201)–P(2)–C(212)	106.2(5)
C(61)–B(6)–B(5)	128.4(9)	C(211)–P(2)–C(212)	100.2(5)
B(6)–C(61)–C(62)	113.9(9)		

In the $^{11}B-\{^1H\}$-NMR spectrum of **3** are five resonances, 1:2:1:4:1, high frequency to low frequency. The highest frequency resonance appears as an unresolved doublet ($^1J_{F-B}$ of ca. 45 Hz) which is unchanged in the proton-coupled spectrum, and therefore arises from the labelled B atom. The integral-4 resonance includes an integral-1 shoulder to the high-frequency side. In the ^{19}F-NMR spectrum is a partially resolved quartet, from which $^1J_{F-B}$ of ca. 39 Hz is measured. The FB coupling constant in **3** compares with those in the *closo* and *nido* precursors 1,2-Ph_2-3-F-1,2-*closo*-$C_2B_{10}H_9$ and [3-F-7,8-Ph_2-7,8-*nido*-$C_2B_9H_9$]$^-$ of ca. 49 and 55 Hz, respectively [8]. The $^{31}P-\{^1H\}$-NMR spectrum is a sharp singlet with Pt satellites ($^1J_{Pt-P}$ = 3259 Hz). Given that **3** is subsequently shown (vide infra) to be isostructural with **2** this implies that the

Table 3
Selected interatomic distances (Å) and interbond angles (°) for **2**

Bond lengths			
Pt(2)–C(1)	2.628(4)	B(7)–B(12)	1.776(6)
Pt(2)–B(3)	2.240(5)	B(7)–B(11)	1.826(6)
Pt(2)–B(7)	2.201(4)	C(8)–B(9)	1.749(6)
Pt(2)–B(11)	2.229(5)	C(8)–B(12)	1.728(6)
Pt(2)–B(6)	2.292(5)	B(9)–B(10)	1.785(7)
C(1)–B(3)	1.678(6)	B(9)–B(12)	1.768(6)
C(1)–B(4)	1.685(6)	B(10)–B(11)	1.763(7)
C(1)–B(5)	1.669(6)	B(10)–B(12)	1.772(7)
C(1)–B(6)	1.735(6)	B(11)–B(12)	1.766(7)
B(3)–B(7)	1.873(6)	B(4)–C(41)	1.576(7)
B(3)–C(8)	1.754(6)	C(41)–C(42)	1.451(9)
B(3)–B(4)	1.855(6)	Pt(2)–P(1)	2.3028(11)
B(4)–C(8)	1.750(6)	Pt(2)–P(2)	2.2925(11)
B(4)–B(9)	1.767(7)	P(1)–C(101)	1.828(4)
B(4)–B(5)	1.759(7)	P(1)–C(111)	1.821(4)
B(5)–B(9)	1.736(8)	P(1)–C(112)	1.819(4)
B(5)–B(10)	1.779(7)	P(2)–C(201)	1.820(4)
B(5)–B(6)	1.835(7)	P(2)–C(211)	1.828(4)
B(6)–B(10)	1.815(7)	P(2)–C(212)	1.811(4)
B(6)–B(11)	1.855(7)	C(1)–C(11)	1.503(6)
B(7)–C(8)	1.721(6)	C(8)–C(81)	1.511(6)
Bond angles			
C(11)–C(1)–Pt(2)	112.0(3)	B(4)–C(41)–C(42)	119.7(5)
C(11)–C(1)–B(3)	122.9(3)	P(1)–Pt(2)–P(2)	96.16(4)
C(11)–C(1)–B(4)	119.2(3)	Pt(2)–P(1)–C(101)	114.45(14)
C(11)–C(1)–B(5)	118.1(3)	Pt(2)–P(1)–C(111)	113.64(15)
C(11)–C(1)–B(6)	119.0(3)	Pt(2)–P(1)–C(112)	118.30(15)
C(81)–C(8)–B(3)	122.6(3)	C(101)–P(1)–C(111)	104.6(2)
C(81)–C(8)–B(7)	115.7(3)	C(101)–P(1)–C(112)	102.0(2)
C(81)–C(8)–B(12)	117.6(3)	C(111)–P(1)–C(112)	102.0(2)
C(81)–C(8)–B(9)	117.7(3)	Pt(2)–P(2)–C(201)	113.31(13)
C(81)–C(8)–B(4)	116.4(3)	Pt(2)–P(2)–C(211)	116.26(15)
C(41)–B(4)–C(1)	122.4(4)	Pt(2)–P(2)–C(212)	117.71(17)
C(41)–B(4)–B(3)	119.7(4)	C(201)–P(2)–C(211)	101.2(2)
C(41)–B(4)–C(8)	122.8(4)	C(201)–P(2)–C(212)	105.2(2)
C(41)–B(4)–B(9)	126.7(4)	C(211)–P(2)–C(212)	101.1(2)
C(41)–B(4)–B(5)	128.7(4)		

$\{PtP_2\}$ unit in **3** is rapidly spinning about the metal-cage axis on the NMR timescale.

Compound **3** crystallises from CH_2Cl_2 in the presence of 40–60 petroleum ether as the solvate $\mathbf{3}\cdot1\frac{3}{4}CH_2Cl_2$, but this loses solvent on standing in air (microanalytical results fit best with 0.6 mol of solvate per platinacarborane). A freshly crystallised sample was subject to crystallographic study. A perspective view of a single molecule of the platinacarborane is shown in Fig. 3, and in Table 4 are selected molecular parameters. The compound is confirmed as 1,8-Ph_2-2,2-$(PMe_2Ph)_2$-4-F-2,1,8-*closo*-$PtC_2B_9H_8$, isostructural with **2**. Thus the Pt atom is slipped, by ca. 0.37 Å, away from C1, rendering Pt–C1 the longest metal-cage atom distance, 2.625(6) Å (cf. Pt–B distances of 2.20–2.29 Å). There is a high degree of congruence between the orientations of the cage-Ph groups in **2** and **3**, and, although this does not extend to the orientations of the phosphine ligands, Pt–P distances and P–Pt–P angles in the two compounds are practically identical.

3.2. Mechanistic implications

We undertook this study as an extension of recent work [9] on the metallation of [3-Et-7,8-Ph_2-7,8-*nido*-$C_2B_9H_8]^{2-}$ with a $\{Ni(dppe)\}^{2+}$ fragment. The nickelation produced not only the expected 1,2 → 1,2 C atom isomerised metallacarborane, but also an (unexpected) 1,2 → 1,7 C atom isomerised species. The position of the Et label in the latter compound did not accord with that anticipated if the (presumed transient) compound 1,2-Ph_2-3-dppe-6-Et-3,1,2-*closo*-$NiC_2B_9H_8$, which would be expected to form first, underwent the same 1,2 → 1,7 C atom isomerisation process predicted for 1,2-*closo*-$C_2B_{10}H_{12}$ [7g]. Instead, the simplest explanation of the observed product, which has a 4-Et-2,1,8-*closo*-NiC_2B_9 architecture, is that it is formed from the transient initial species by rotation of a CB_2 triangular face [9].

In the present case, similar 4-X-2,1,8-*closo*-PtC_2B_9 geometries are displayed by compounds **2** (X = Et) and **3** (X = F), which can therefore be rationalised by the same CB_2 triangle face mechanism, shown in Scheme 1. To try to gain further insight into the precise isomerisation mechanism operating, experiments are currently in hand in which B atoms in this CB_2 face are additionally

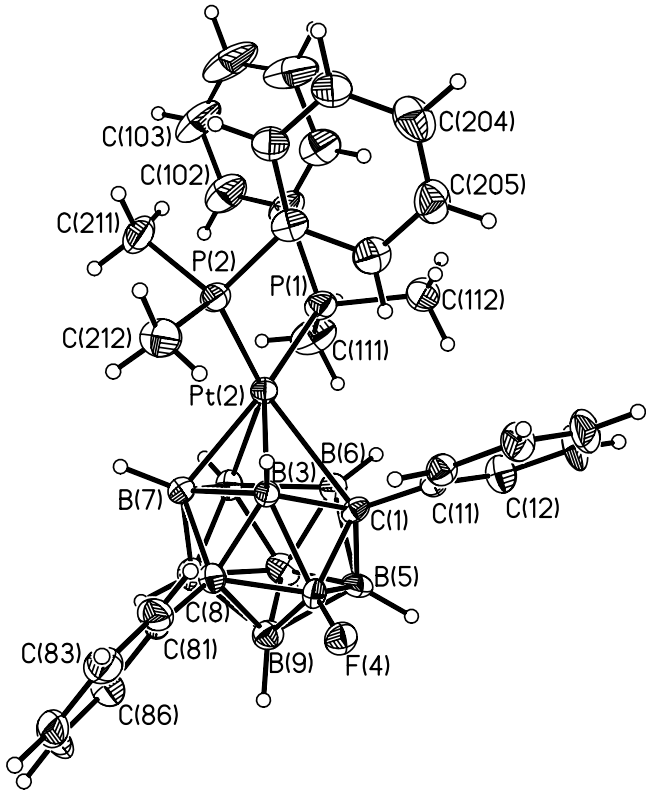

Fig. 3. Perspective view of compound **3**. Thermal ellipsoids are drawn at the 50% probability level, except for H atoms.

Table 4
Selected interatomic distances (Å) and interbond angles (°) for **3**·1¾CH_2Cl_2

Bond lengths			
Pt(2)–C(1)	2.625(6)	B(7)–B(12)	1.778(10)
Pt(2)–B(3)	2.216(6)	B(7)–B(11)	1.797(10)
Pt(2)–B(7)	2.206(7)	C(8)–B(9)	1.770(9)
Pt(2)–B(11)	2.222(7)	C(8)–B(12)	1.731(9)
Pt(2)–B(6)	2.281(7)	B(9)–B(10)	1.787(10)
C(1)–B(3)	1.669(8)	B(9)–B(12)	1.751(10)
C(1)–B(4)	1.624(9)	B(10)–B(11)	1.777(11)
C(1)–B(5)	1.682(9)	B(10)–B(12)	1.787(10)
C(1)–B(6)	1.747(8)	B(11)–B(12)	1.770(10)
B(3)–B(7)	1.854(10)	B(4)–F(4)	1.351(8)
B(3)–C(8)	1.742(9)	Pt(2)–P(1)	2.2982(17)
B(3)–B(4)	1.841(9)	Pt(2)–P(2)	2.2893(16)
B(4)–C(8)	1.733(9)	P(1)–C(101)	1.829(7)
B(4)–B(9)	1.773(10)	P(1)–C(111)	1.808(8)
B(4)–B(5)	1.749(10)	P(1)–C(112)	1.813(7)
B(5)–B(9)	1.751(10)	P(2)–C(201)	1.824(7)
B(5)–B(10)	1.784(10)	P(2)–C(211)	1.815(7)
B(5)–B(6)	1.827(10)	P(2)–C(212)	1.835(7)
B(6)–B(10)	1.800(10)	C(1)–C(11)	1.498(8)
B(6)–B(11)	1.857(10)	C(8)–C(81)	1.513(8)
B(7)–C(8)	1.700(9)		
Bond angles			
C(11)–C(1)–Pt(2)	112.3(4)	F(4)–B(4)–B(5)	128.1(5)
C(11)–C(1)–B(3)	121.2(5)	P(1)–Pt(2)–P(2)	96.87(6)
C(11)–C(1)–B(4)	118.4(5)	Pt(2)–P(1)–C(101)	119.4(2)
C(11)–C(1)–B(5)	118.4(5)	Pt(2)–P(1)–C(111)	113.0(3)
C(11)–C(1)–B(6)	121.4(5)	Pt(2)–P(1)–C(112)	103.4(3)
C(81)–C(8)–B(3)	121.3(5)	C(101)–P(1)–C(111)	102.6(4)
C(81)–C(8)–B(7)	119.6(5)	C(101)–P(1)–C(112)	103.4(3)
C(81)–C(8)–B(12)	120.4(5)	C(111)–P(1)–C(112)	103.3(4)
C(81)–C(8)–B(9)	116.0(5)	Pt(2)–P(2)–C(201)	116.8(2)
C(81)–C(8)–B(4)	113.3(5)	Pt(2)–P(2)–C(211)	113.4(3)
F(4)–B(4)–C(1)	123.2(5)	Pt(2)–P(2)–C(212)	115.4(2)
F(4)–B(4)–B(3)	119.6(5)	C(201)–P(2)–C(211)	105.2(3)
F(4)–B(4)–C(8)	119.9(5)	C(201)–P(2)–C(212)	102.7(3)
F(4)–B(4)–B(9)	123.8(6)	C(211)–P(2)–C(212)	101.6(4)

labelled, and the results of these studies will be published separately [22].

Finally, we comment on the isolation of the non-isomerised species **1**, which has no precedent in the nickelation reactions. We believe this may be linked to the greater electronic preference of $\{PtP_2\}$ fragments to undergo slipping distortions in 3,1,2-*closo*-MC_2B_9 species [15] relative to similar nickel fragments [10]. By slipping away from C1 and C2, the $\{Pt(PMe_2Ph)_2\}$ fragment avoids to some degree unfavourable steric crowding, and hence the need to isomerise, in a way that a {Ni(dppe)} fragment cannot. The fact that **1** transforms into **2** on gentle heating confirms that the former is only kinetically preferred. The subtle interplay between electronic and steric preferences in these metallacarboranes affords them a considerably greater degree of complexity and interest than their much more simple carborane cousins, and is appropriate testimony to the pioneering work of Hawthorne et al. [3] nearly 40 years ago.

4. Supplementary material

Crystallographic data for the structural analyses have been deposited with the Cambridge Crystallographic Data Centre, CCDC Nos. 204400 (**1**), 204401 (**2**) and 204402 (**3**·1¾CH_2Cl_2). Copies of this information may be obtained free of charge from The Director, CCDC, 12 Union Road, Cambridge, CB2 1EZ, UK (Fax: +44-1233-336-033; e-mail: deposit@ccdc.cam.ac.uk or www: http://www.ccdc.cam.ac.uk).

Acknowledgements

We thank the Leverhulme Trust (DE) and Heriot-Watt University (SR) for support, Mr G. Evans and Mrs. C. Graham for microanalysis and Dr A.S.F. Boyd for NMR spectra. A.J.W. acknowledges the receipt of a Royal Society Leverhulme Trust Senior Research Fellowship, 2002–2003.

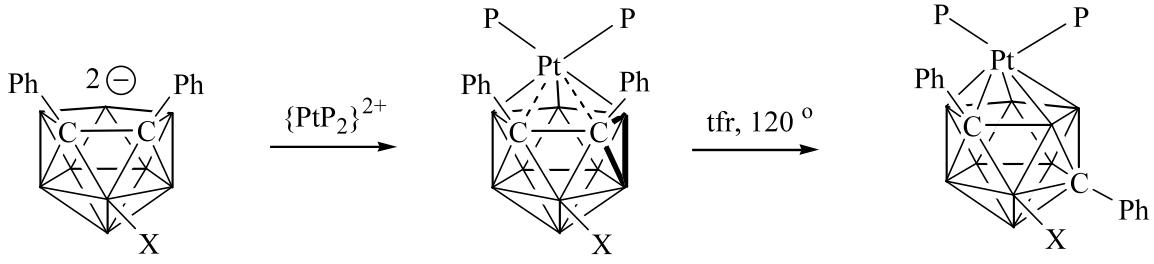

[3-X-7,8-Ph_2-7,8-*nido*-$C_2B_9H_8$]$^{2-}$ transient 1,8-Ph_2-4-X-2,1,8-*closo*-$PtC_2B_9H_8$

Scheme 1. Metallation of [3-X-7,8-Ph_2-7,8-*nido*-$C_2B_9H_8$]$^{2-}$ with a $\{Pt(PMe_2Ph)_2\}^{2+}$ fragment (abbreviated to $\{PtP_2\}^{2+}$ for clarity) generating a 4-X-labelled C-atom isomerised 2,1,8-PtC_2B_9 species via rotation of the (bold) CB_2 face of a notional 6-X-3,1,2-PtC_2B_9 intermediate. Compound **1** corresponds to the intermediate and compounds **2** and **3** to the final product.

References

[1] D. Grafstein, J. Dvorak, Inorg. Chem. 2 (1963) 1128.
[2] L.I. Zakharkin, V.N. Kalinin, Izv. Akad. Nauk SSSR, Ser. Khim. (1969) 607.
[3] M.F. Hawthorne, D.C. Young, P.A. Wegner, J. Am. Chem. Soc. 87 (1965) 1818.
[4] R. Hoffmann, Angew. Chem. Int. Ed. 21 (1982) 711.
[5] D.R. Baghurst, R.C.B. Copley, H. Fleischer, D.M.P. Mingos, G.O. Kyd, L.J. Yellowlees, A.J. Welch, T.R. Spalding, D. O'Connell, J. Organometal. Chem. 447 (1993) C14.
[6] (a) A.J. Welch, Steric effects in metallacarboranes, in: P. Braunstein, L.A. Oro, P.R. Raithby (Eds.), Metal Clusters in Chemistry, Wiley/VCH, New York/Weinheim, 1999, p. 69 (and references therein);
(b) G. Barberà, S. Dunn, M.A. Fox, R.M. Garrioch, B.E. Hodson, K.S. Low, G.M. Rosair, F. Teixidor, C. Viñas, A.J. Welch, A.S. Weller, Towards experimental mapping of the mechanism of heteroborane isomerisation, in: M.G. Davidson, A.K. Hughes, T.B. Marder, K. Wade (Eds.), Contemporary Boron Chemistry, Royal Society of Chemistry, 2000, p. 329 (and references therein).
[7] (a) W.N. Lipscomb, Science 153 (1966) 373;
(b) H.D. Kaeze, R. Bau, H.A. Beal, W.N. Lipscomb, J. Am. Chem. Soc. 86 (1967) 4218;
(c) L.I. Zakharkin, V.N. Kalinin, Dokl. Akad. Nauk SSSR 169 (1966) 590;
(d) S.-H. Wu, M. Jones, J. Am. Chem. Soc. 111 (1989) 5373;
(e) H.S. Wong, W.N. Lipscomb, Inorg. Chem. 14 (1975) 1350;
(f) G.M. Edvenson, D.F. Gaines, Inorg. Chem. 29 (1990) 1210;
(g) D.J. Wales, J. Am. Chem. Soc. 115 (1993) 1557.
[8] S. Robertson, D. Ellis, T.D. McGrath, G.M. Rosair, A.J. Welch, Polyhedron 22 (2003) 1293.
[9] S. Robertson, D. Ellis, G.M. Rosair, A.J. Welch, Appl. Organometal. Chem. 17 (2003) 516.
[10] R.M. Garrioch, P. Kuballa, K.S. Low, G.M. Rosair, A.J. Welch, J. Organometal. Chem. 575 (1999) 57.
[11] J.M. Jenkins, B.L. Shaw, J. Chem. Soc. A (1966) 770.
[12] Siemens Analytical Instruments, Inc., Madison, WI, 1996.
[13] G.M. Sheldrick, SHELXTL Version 5.1, Bruker AXS, Inc., Madison, WI, 1999.
[14] A.S. Weller, A.J. Welch, J. Chem. Soc. Dalton Trans. (1997) 1205.
[15] D.M.P. Mingos, M.I. Forsyth, A.J. Welch, J. Chem. Soc. Dalton Trans. (1978) 1363.
[16] Compare 10-*endo*-Ph_3PHg-7,8-*nido*-$C_2B_9H_{11}$ [Δ 0.92 Å; H.M. Colquhoun, T.J. Greenhough, M.G. Wallbridge, J. Chem. Soc. Dalton Trans. (1979) 619] with 7,8-Ph_2-10-*endo*-Ph_3PHg-7,8-*nido*-$C_2B_9H_9$ [Δ 1.10 Å; Z.G. Lewis, A.J. Welch, Acta Crystallogr. C 49 (1993) 715] and 3-(η^2: η^2-1,5-cod)-3,1,2-*closo*-$PdC_2B_9H_{11}$ [Δ 0.24 Å; D.E. Smith, A.J. Welch, Acta Crystallogr. C 42 (1986) 1717] with 1,2-Ph_2-3-(η^2: η^2-1,5-cod)-3,1,2-*closo*-$PdC_2B_9H_9$ [Δ 0.52 Å; G.O. Kyd, L.J. Yellowlees, A.J. Welch, J. Chem. Soc. Dalton Trans. (1994) 3129].
[17] J. Cowie, B.D. Reid, J.M.S. Watmough, A.J. Welch, J. Organometal. Chem. 481 (1994) 283.
[18] (a) Z.G. Lewis, A.J. Welch, J. Organometal. Chem. 430 (1992) C45;
(b) P.T. Brain, M. Bühl, J. Cowie, Z.G. Lewis, A.J. Welch, J. Chem. Soc. Dalton Trans. (1996) 231;
(c) U. Grädler, A.S. Weller, A.J. Welch, D. Reed, J. Chem. Soc. Dalton Trans. (1996) 335;
(d) A.J. Welch, A.S. Weller, Inorg. Chem. 35 (1996) 4548;
(e) G.M. Rosair, A.J. Welch, A.S. Weller, Organometallics 17 (1998) 3227;
(f) M.A. McWhannell, G.M. Rosair, A.J. Welch, F. Teixidor, C. Viñas, J. Organometal. Chem. 573 (1999) 165;
(g) D. Reed, A.J. Welch, J. Cowie, D.J. Donohoe, J.A. Parkinson, Inorg. Chim. Acta 289 (1999) 125.
[19] J. Cowie, D.J. Donohoe, N.L. Douek, A.J. Welch, Acta Crystallogr. C 49 (1993) 710.
[20] Z.G. Lewis, A.J. Welch, Acta Crystallogr. C 49 (1993) 705.
[21] G.O. Kyd, Ph.D. Thesis, University of Edinburgh, 1996.
[22] T.L. Sadler, D. Ellis, R.M. Garrioch, G.M. Rosair, A.J. Welch, in preparation.